RESEARCH ARTICLE

Diffusion weighted imaging combining respiratory triggering and navigator echo tracking in the upper abdomen

Yoshihiko Tachikawa[1] · Hiroshi Hamano[2] · Naoya Chiwata[1] · Hikaru Yoshikai[1] · Kento Ikeda[1] · Yasunori Maki[1] · Yukihiko Takahashi[3] · Makiko Koike[3]

Abstract

Objectives To evaluate a new motion correction method, named RT + NV Track, for upper abdominal DWI that combines the respiratory triggering (RT) method using a respiration sensor and the Navigator Track (NV Track) method using navigator echoes.

Materials and methods To evaluate image quality acquired upper abdominal DWI and ADC images with RT, NV, and RT + NV Track in 10 healthy volunteers and 35 patients, signal-to-noise efficiency ($SNR_{efficiency}$) and the coefficient of variation (CV) of ADC values were measured. Five radiologists independently performed qualitative image-analysis assessments.

Results RT + NV Track showed significantly higher $SNR_{efficiency}$ than RT and NV (14.01 ± 4.86 vs 12.05 ± 4.65, 10.05 ± 3.18; $p < 0.001$, $p < 0.001$). RT + NV Track was superior to RT and equal or better quality than NV in CV and visual evaluation of ADC values (0.033 ± 0.018 vs 0.080 ± 0.042, 0.057 ± 0.034; $p < 0.001$, $p < 0.001$). RT + NV Track tends to acquire only expiratory data rather than NV, even in patients with relatively rapid breathing, and can correct for respiratory depth variations, a weakness of RT, thus minimizing image quality degradation.

Conclusion The RT + NV Track method is an efficient imaging method that combines the advantages of both RT and NV methods in upper abdominal DWI, providing stably good images in a short scan time.

Keywords Diffusion weighted imaging · Respiratory triggering · Navigator echo tracking · Abdomen · Motion correction · Apparent diffusion coefficient

Introduction

Abdominal diffusion weighted imaging (DWI) has proven clinically useful in lesion detection and follow-up due to lesion conspicuity and non-invasive nature without contrast enhancement [1–3]. DWI has been found to be useful in detecting primary hepatic malignancies such as hepatocellular carcinoma and cholangiocarcinoma [4, 5],

and DWI has been incorporated into clinical guidelines such as the Liver Imaging Reporting and Data System (LI-RADS) [6]. In the liver, DWI is also useful for detecting small lesions around blood vessels and in the periphery of the liver that are difficult to detect on T2-weighted images [7, 8]. Therefore, DWI is recommended as an essential image to detect liver metastases from colorectal, pancreatic, and neuroendocrine primary lesions [1, 9, 10]. This means that abdominal DWI is an essential sequence that improves the sensitivity of MRI for detecting neoplastic lesions. In addition, based on the calculation of apparent diffusion coefficient (ADC), DWI enables the characterization of biological tissues based on water diffusion properties determined by the microstructural organization, cell density, and viability of the tissues [11]. However, DWI of the upper abdomen is highly sensitive to physiologic motions such as respiration. When patients' respiration varies due to anxiety, tremor, or poor tolerance, ghosting and blurring artifacts may occur, resulting in poor

✉ Yoshihiko Tachikawa
  yoshihiko-tachikawa@karatsu.jrc.or.jp

1 Division of Radiological Technology, Department of Medical Technology, Karatsu Red Cross Hospital, 2430 Watada, Karatsu, Saga 847-8588, Japan

2 Philips Japan, Philips Building, 2-13-37 Kohnan, Minato-ku, Tokyo 108-8507, Japan

3 Department of Radiology, Karatsu Red Cross Hospital, 2430 Watada, Karatsu, Saga 847-8588, Japan

image quality and inaccurate quantification of the ADC, which may lead to erroneous diagnoses [12]. Therefore, several motion corrections in DWI have been reported to suppress the influence of respiratory-induced misregistration artifacts, but each method has several problems.

First, the simplest approach is the breath-hold (BH) method using single-shot-EPI with a single breath-hold [12–17]. Choi et al. [18] used the BH method to shorten the scan time, reduce the effect of physiologic motion, and improve the detection of small local liver lesions. However, compared to the non-breath-hold method, the single BH method has a lower SNR due to the limitation of scan time [12, 13]. In particular, the BH method was reported to have significantly lower SNR for the liver and lesions at both lower b values ($b = 50$) and higher b values ($b = 800$) than the non-breath-hold method at 3.0 T, and the CNR of the lesions was also significantly lower [18]. Moreover, because higher SNR and higher spatial resolution are required for abdominal DWI, multiple breath-holds must be performed for higher averaging, resulting in the inevitable possibility of respiratory-induced misregistration, often making accurate ADC measurements difficult. Second, the free-breathing (FB) method, which averages respiratory motion

by increasing the number of signals averages, makes the scan time or acquisition interval independent of variations in the respiratory cycle during acquisition. Therefore, the FB method is more time-efficient than the navigator-triggered (NV) and respiratory-trigger (RT) methods [18–20]. The FB method has also been reported to have good reproducibility in ADC measurement of liver parenchyma [19, 21]. On the other hand, the FB method has a noticeable blurring due to respiration, and the sharpness of the image is not as good as that of the NV or RT methods [12, 22]. Furthermore, since all data is acquired from inspiration to expiration, accurate ADC images are difficult to be obtained due to respiratory-induced misregistration between low b-values ($0 \sim 100$ s/mm^2) and high b-values ($800 \sim 1000$ s/mm^2). In particular, large differences in ADC values between slices are often observed (Fig. 1A; Supporting Information Video S1). Increasing the number of signals averages to reduce these influences increases scan time. Third, the RT method uses an air-filled pressure sensor with a breathing belt to constantly track the respiratory phase [13, 23–25]. With this approach, images of the same respiratory phase are acquired and averaged to obtain a high SNR image. Therefore, the RT method provides higher sharpness and
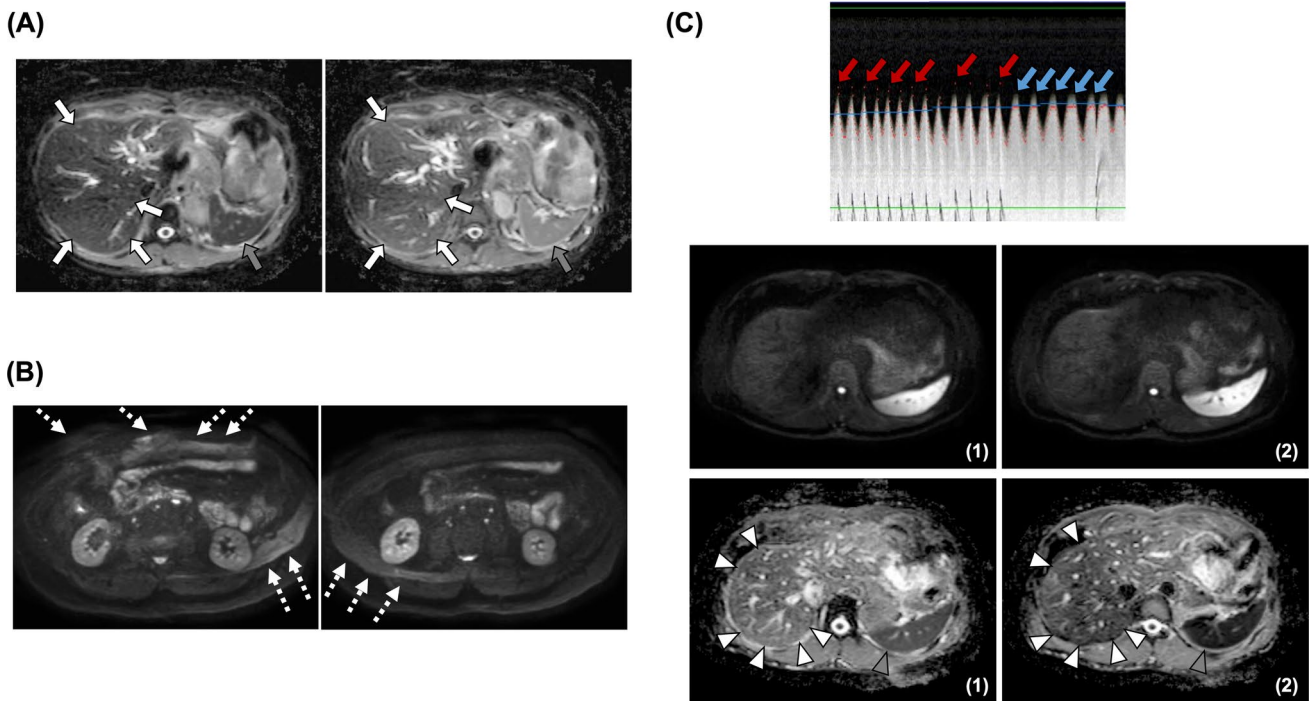
Fig. 1 Problems with conventional motion correction methods in DWI. In the free-breathing (FB) method (**A**), respiratory-induced misregistration often causes uneven signal intensity on the liver (arrows) and spleen (gray arrows) between slices of the ADC image. In the respiratory triggered (RT) method (**B**), poor fat suppression often occurs in the initial slices of excitation, degrading image quality as artifacts (dashed arrows). In the navigator-triggered (NV) method

(**C**), magnetic field inhomogeneity sometimes causes poor navigator readings (red arrows) that raise the triggering position (blue line), resulting in no data acquisition or inclusion of inspiratory data in the data acquisition (blue arrows). Consequently, DWI image quality degradation and significant uneven signal intensity between slices in the ADC image (arrowheads, gray arrowheads) are caused

lesion-liver contrast than the FB method [24] and higher SNR images than the BH method [13, 25]. However, the RT method is prone to image quality degradation and slice misregistration between multiple *b* values due to variations in the depth of respiration (Supporting Information Video S2 and Fig. S1). Additionally, poor fat suppression often occurs in the initial slice of excitation (Fig. 1B). Fourth, another approach to reduce motion artifacts due to respiration is the NV method, in which the position of the diaphragm is constantly measured by the navigator and used to trigger the scan [26–28]. Compared to the BH method, the NV method has been shown to provide less misregistration of slices due to variations in the depth of respiration, more accurate ADC measurements, and improved SNR, CNR, image quality, and lesion detection [26, 28]. Furthermore, the NV method has been reported to be superior to the FB and BH methods in the sharpness of the liver at 3.0 T [22]. However, poor navigator readings due to magnetic field inhomogeneity can cause inaccurate triggering, resulting in poor image quality and increased scan time due to the inability to acquire data (Fig. 1C). In addition, patients with rapid breathing often experience delays in navigator triggering, resulting in poor image quality due to the inclusion of inspiratory data in the data acquisitions [Fig. 1C; Supporting Information Video S3].

Here, we propose a new motion correction method in upper abdominal DWI that combines the RT method using a respiration sensor and the Navigator Track (NV Track) method using navigator echoes to correct for respiratory variations in the diaphragm position. This method may improve the image quality degradation caused by variations in the depth of respiration in the RT method and the image quality degradation and increased scan time caused by poor navigator readings in the NV method. In this study, we evaluated the image quality of the new motion correction method named RT + NV Track (respiratory triggering and navigator echo tracking) compared to the conventional motion correction methods, RT and NV, in upper abdominal DWI.

Material and methods

### Motion correction technique

The specifications of each motion correction technique considered in this study are as follows. The conventional RT method uses an air-filled pressure sensor with a breathing belt on the abdomen to read the movement of the abdominal wall. Data acquisition is triggered at 50% from maximal inspiration and after an appropriate trigger delay time that is set in order to allow data acquisition to be repeated during expiration (Fig. 2A). However, a concern is that

the RT method is susceptible to variations in the depth of respiration (Supporting Information Video S2 and Fig. S1). The conventional NV (Trigger and track) method reads the movement of the diaphragm in the prescan, automatically sets the trigger to the position of the diaphragm at expiration (blue line), and data acquisition is performed at expiration beyond the blue line of the trigger (Fig. 2B). In addition, the navigator constantly reads the position of the diaphragm and tracks changes in the position of the diaphragm due to respiratory variations. However, a concern is that the NV method may cause inaccurate setting of the trigger position due to poor navigator reading caused by inhomogeneity of the magnetic field (Fig. 1C). The motion correction technique of the proposed RT + NV Track method is a combination of the RT method using a respiration sensor and the NV Track method using navigator echoes. First, the appropriate trigger delay time is set according to the respiratory waveform of each subject, as in the RT method, which is a conventional motion correction method (Fig. 2A). Data acquisitions start after the set trigger delay time, but just before that time, NV Track is operated to correct the slice position misregistration due to respiratory variations at the diaphragm position (Fig. 2C). Therefore, the data is actually acquired at the slice position corrected by the NV Track. The proposed RT + NV Track method can be used by changing some parameters in the clinical product.

Experiments

All images were acquired on a 3 T MR scanner (Ingenia, Philips Healthcare, Best, the Netherlands) using a 32-channel anterior and posterior phased-array coil. Upper abdominal DWI images with RT, NV, and RT + NV Track were acquired in 10 healthy volunteers (7 men, 3 women; age range 24–54 years [mean age 37.6 ± 12.2 years]; weight range 52–100 kg [mean weight 60.4 ± 17.8 kg]) without known diseases. In addition, upper abdominal DWI images with RT, NV, and RT + NV Track were also acquired in 35 patients (17 men, 18 women; age range 43–95 years [mean age 71.1 ± 11.2 years]; weight range 37–84 kg [mean weight 58.6 ± 11.8 kg]): 11 with hepatocellular carcinoma, 8 with liver metastases, 7 with liver hemangioma, 6 with pancreatic cancer, and 3 with suspected gallbladder polyps or stones. All subjects were examined with a respiratory belt to minimize respiratory movements.

The detailed imaging parameters are given in Table 1. The same image acquisition was performed for each triggering session for the RT, NV, and RT + NV Track methods. Since we set the Package to 2, b0 images of odd slices such as [1, 3, 5, 7, 9, …] were first acquired sequentially for each respiration. Then, b1000 images of odd slices were sequentially acquired. Next, b0 and b1000 images of even slices such as [2, 4, 6, 8, 10,…] were sequentially acquired

(A)

(B)

(C)
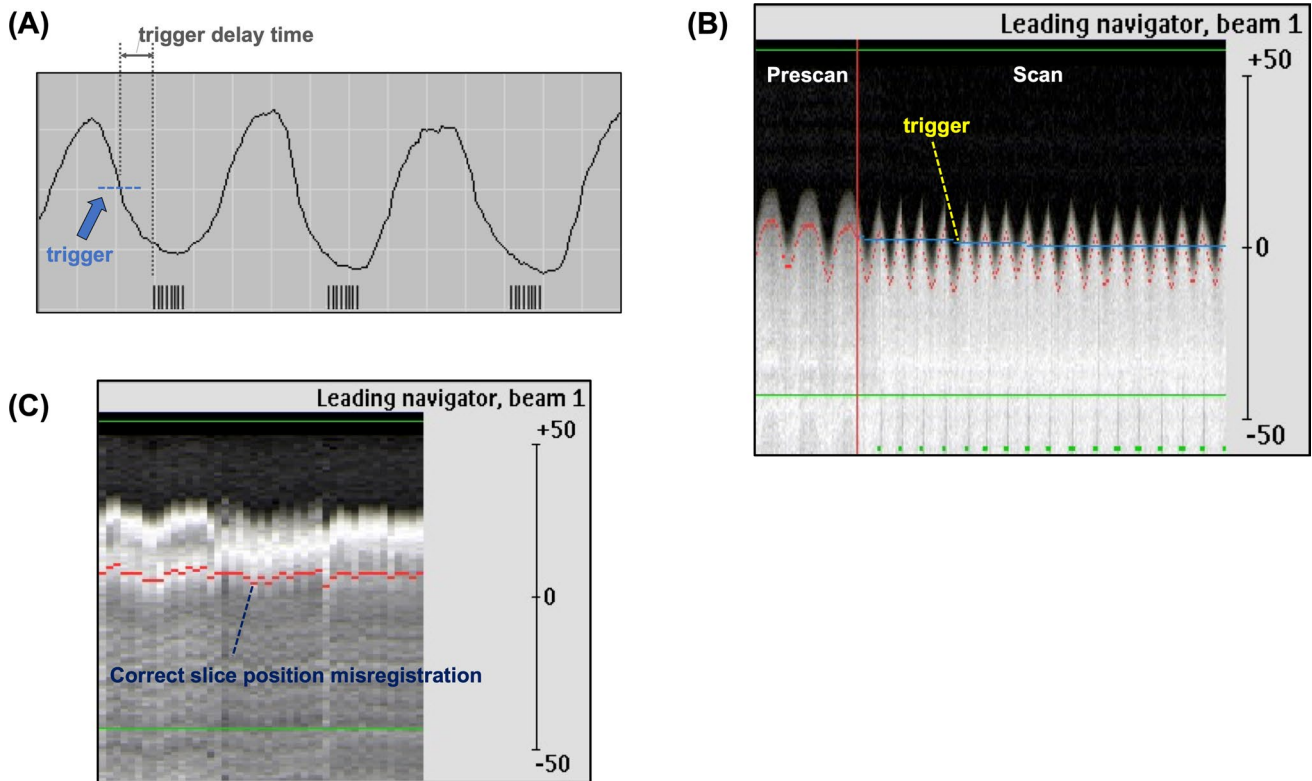
Fig. 2 The RT method is triggered at 50% of the respiratory waveform from maximal inspiration (blue arrow) and collects expiratory data by setting the appropriate trigger delay time for each subject's respiratory waveform (**A**). The NV (Trigger and track) method reads the movement of the diaphragm in the prescan and automatically sets the trigger to the position of the diaphragm at expiration (blue line). Data acquisition is performed at expiration beyond the blue line of the trigger (**B**). In addition, the navigator constantly reads the position of the diaphragm and tracks changes in the position of the diaphragm due to respiratory variations (**B**). The RT+NV Track method is a combination of the RT and NV Track methods. As with the RT method, the appropriate trigger delay time for each subject's respiratory waveform is set so that data collection occurs at expiration (**A**). In addition, Navigator Track (NV Track) is performed just before data acquisition to correct the misregistration of the slice position due to respiratory variation at the diaphragm position (**B**). Actually, the slice position corrected by NV Track is acquired

for each respiration in the same way as the odd slices. In other words, b0 images of Package1 (odd slices) were first acquired with the number of respirations for the number of odd slices x NSA, and then b1000 images of Package1 (odd slices) were acquired with the number of respirations for the number of odd slices x diffusion-encoded axes x NSA. Next, Package2 (even slices) was also acquired in the same way as Package1 (odd slices).

Quantitative image analysis

We placed circular regions of interest (ROIs, 100 mm^2) at four points on the liver of DWI (b1000) images and measured the mean signal intensity (SI) and SD of the signal intensity (Fig. 3A). Then, the SNR of the four ROIs on the liver was calculated by SNR = mean SI_{liver}/SD_{liver}, and $SNR_{efficiency}$ was calculated as previously reported [29] with the following formula:

$$SNR_{efficiency} = SNR/\sqrt{Actual\ scan\ time}.$$

To minimize bias due to single measurements, we placed these ROIs on three sequential slices and calculated their mean value.

Next, we placed ROIs (80 mm^2) on the right lobe of the liver in four sequential slices of ADC images and measured the mean and SD of the ADC values (Fig. 3B). Then, to evaluate the variation of ADC values on the liver between slices due to respiratory variation, the coefficient of variation (CV) of ADC values on the liver of four sequential slices was calculated using the following formula:

$$CV = SD/mean\ of\ ADC\ values\ of\ 4\ slices$$

To minimize bias due to single measurements, we measured at four points per slice in the right lobe of the liver. There have been reports that cardiac motion artifacts

Table 1 Imaging parameters of the DWI sequences used in the present study

	RT	RT+NV track	NV
FOV [mm^2]	360×320		
Voxel size (ACQ) [mm^3]	3.21×2.14×7.0		
TR/TE [ms]	Shortest (1234)/shortest (73)	Shortest (1278)/shortest (73)	Shortest (1234)/shortest (73)
SENSE reduction	2.5		
Half scan (factor)	0.802		
Fat suppression	SPIR		
SSGR	Yes		
b-factors	0,1000		
Respiratory/navigator	Trigger (RT)	Trigger (RT) & track (NV)	Trigger & track (NV)
Packages	2		
NSA	2		
Scan duration (setting)	2 m 06 s		

RT respiratory triggering, *NV* navigator, *ACQ* acquired, *SPIR* spectral presaturation with inversion recovery, *SSGR* slice-selection gradient reversal, *NSA* number of signal average

(A)

(B)

slice encoding
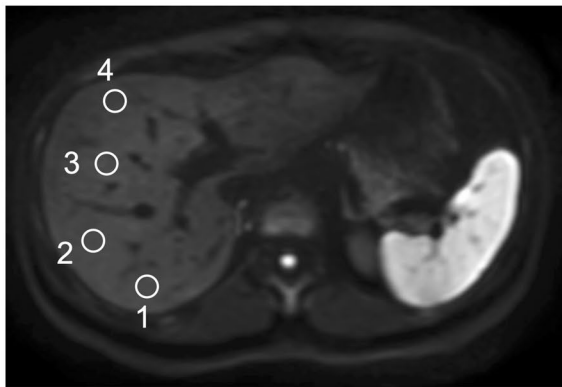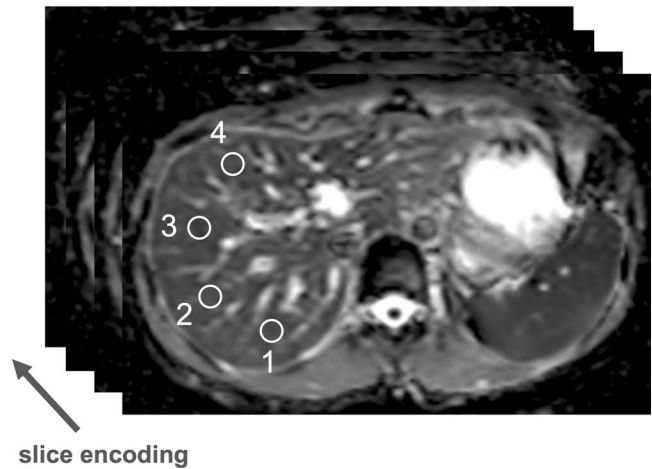
Fig. 3 ROIs placement in quantitative image analysis. **A** To calculate SNR$_{efficiency}$, circular ROIs were placed at four points on the liver on the DWI (b1000) images. **B** To calculate the coefficient of variation (CV) of ADC values of the liver between slices, four circular ROIs per slice were placed on the right lobe of the liver in four sequential slices of the ADC images

and susceptibility artifacts due to stomach contents cause signal degradation and increased ADC values in the left lobe of the liver, leading to reduced detectability of lesions and decreased reliability of ADC measurements in the left lobe of the liver [30–33]. Therefore, we excluded the left lobe of the liver from the measurement points in this study for accurate comparisons of respiratory correction techniques. Wilcoxon signed-rank test was used to compare the quantitative analysis of the RT+NV Track and conventional methods. P values < 0.05 were considered to indicate a significant difference.

Qualitative image analysis

Upper abdominal DWI and ADC images with RT, NV, and RT+NV Track were qualitatively assessed by five radiologists with more than 10 years of experience with MRI. These image data sets were randomized, and observers

were blinded to the acquisition parameters. They scored overall image quality on a 4-point scale (1 [poor], 2 [fair], 3 [good], 4 [excellent]). Wilcoxon signed-rank test was used to compare the qualitative analysis of the RT + NV Track and conventional methods. P-values < 0.05 were considered to indicate a significant difference.
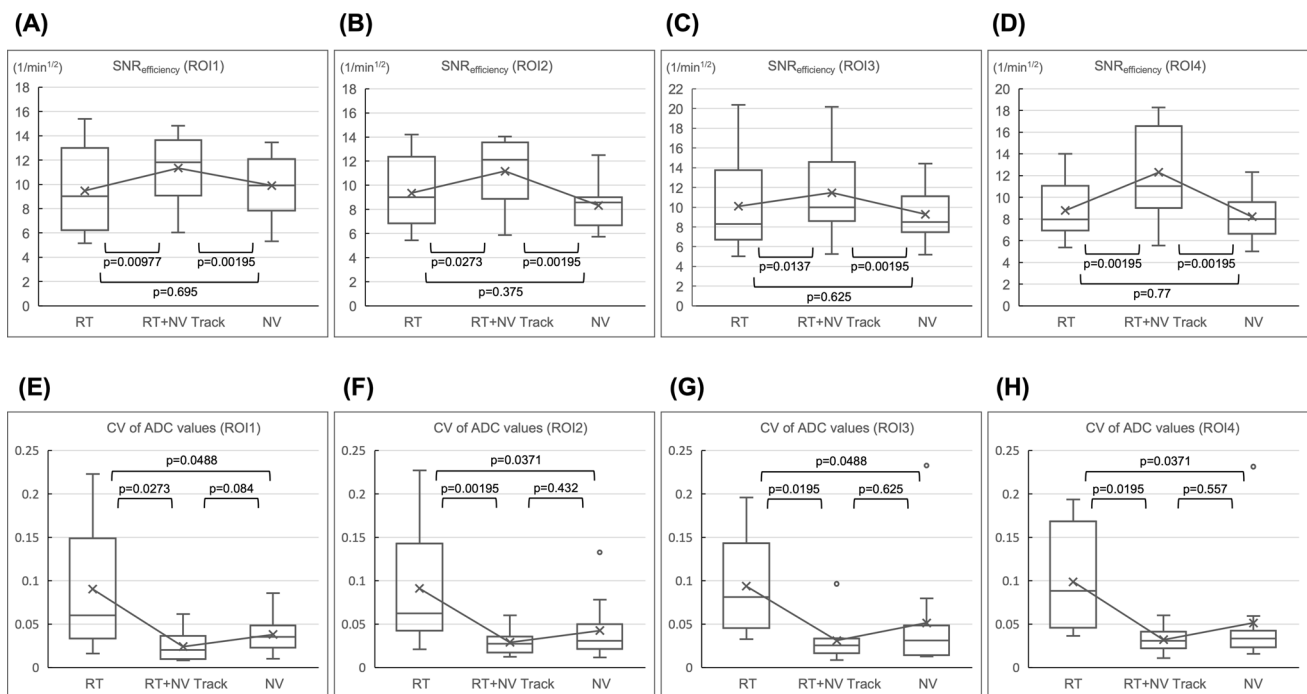
Results

Volunteer study

All data were successfully acquired. RT + NV Track and RT were comparable in actual imaging time (170 ± 24.95 s vs 175.5 ± 30.40 s; $p = 1$). In contrast, RT + NV Track was significantly shorter than NV in actual imaging time (170 ± 24.95 s vs 204.6 ± 37.65 s; $p < 0.01$). The results of the quantitative image analysis are shown in Fig. 4A–D.

In $SNR_{efficiency}$, there was no significant difference between RT and NV in all four ROIs of the liver ([ROI1] 9.48 ± 3.52 $1/min^{1/2}$ vs 9.90 ± 2.58 $1/min^{1/2}$; $p = 0.695$, [ROI2] 9.35 ± 3.06 $1/min^{1/2}$ vs 8.33 ± 1.94 $1/min^{1/2}$; $p = 0.375$, [ROI3] 10.10 ± 4.76 $1/min^{1/2}$ vs 9.28 ± 2.66 $1/min^{1/2}$; $p = 0.625$, [ROI4] 8.78 ± 2.67 $1/min^{1/2}$ vs 8.22 ± 2.35

$1/min^{1/2}$; $p = 0.77$). RT + NV Track was significantly higher than RT and NV in all four ROIs of the liver ([ROI1] 11.34 ± 2.73 $1/min^{1/2}$; $p < 0.01$, $p < 0.01$, [ROI2] 11.17 ± 2.63 $1/min^{1/2}$; $p < 0.05$, $p < 0.01$, [ROI3] 11.47 ± 4.34 $1/min^{1/2}$; $p < 0.05$, $p < 0.01$, [ROI4] 12.30 ± 4.24 $1/min^{1/2}$; $p < 0.01$, $p < 0.01$) (Fig. 4A–D).

In the CV of ADC values, RT + NV Track was significantly lower than RT in all four points of the liver ([ROI1] 0.024 ± 0.018 vs 0.090 ± 0.074; $p < 0.05$, [ROI2] 0.029 ± 0.015 vs 0.091 ± 0.071; $p < 0.01$, [ROI3] 0.031 ± 0.024 vs 0.094 ± 0.057; $p < 0.05$, [ROI4] 0.032 ± 0.014 vs 0.099 ± 0.064; $p < 0.05$). On the other hand, RT + NV Track had lower CV than NV in all four points of the liver, but the difference was not significant ([ROI1] 0.024 ± 0.018 vs 0.038 ± 0.022; $p = 0.084$, [ROI2] 0.029 ± 0.015 vs 0.043 ± 0.037; $p = 0.432$, [ROI3] 0.031 ± 0.024 vs 0.051 ± 0.067; $p = 0.625$, [ROI4] 0.032 ± 0.014 vs 0.051 ± 0.064; $p = 0.557$). (Fig. 4E–H).

The results of the qualitative image analysis are shown in Fig. 5A, B. Moreover, the results of qualitative image analysis are shown below as (Median value [Minimum value—Maximum value], Mode value). In the evaluation of DWI (b1000) images, RT + NV Track was significantly higher than RT (4 [2−4], 4 vs 2.5 [1 − 4], 2; $p < 0.01$).

Fig. 4 Quantitative image analysis results of the volunteer study. In DWI(b1000) images, the SNRefficiency of RT + NV Track was significantly higher than RT and NV in all ROI1 (**A**), ROI2 (**B**), ROI3 (**C**), and ROI4 (**D**) ([ROI1] $p = 0.00977$, 0.00195, [ROI2] $p = 0.0273$, 0.00195, [ROI3] $p = 0.0137$, 0.00195, [ROI4] $p = 0.00195$, 0.00195). There was no significant difference in SNRefficiency between RT and NV in all four ROIs. In CV of ADC values, RT + NV Track and NV were significantly lower than RT in all ROI1 (**E**), ROI2 (**F**), ROI3 (**G**), and ROI4 (**H**) ([ROI1] $p = 0.0273$, 0.0488, [ROI2] $p = 0.00195$, 0.0371, [ROI3] $p = 0.0195$, 0.0488, [ROI4] $p = 0.0195$, 0.0371). The CV of ADC values for RT + NV Track was lower than NV in all four ROIs, but the difference was not significant
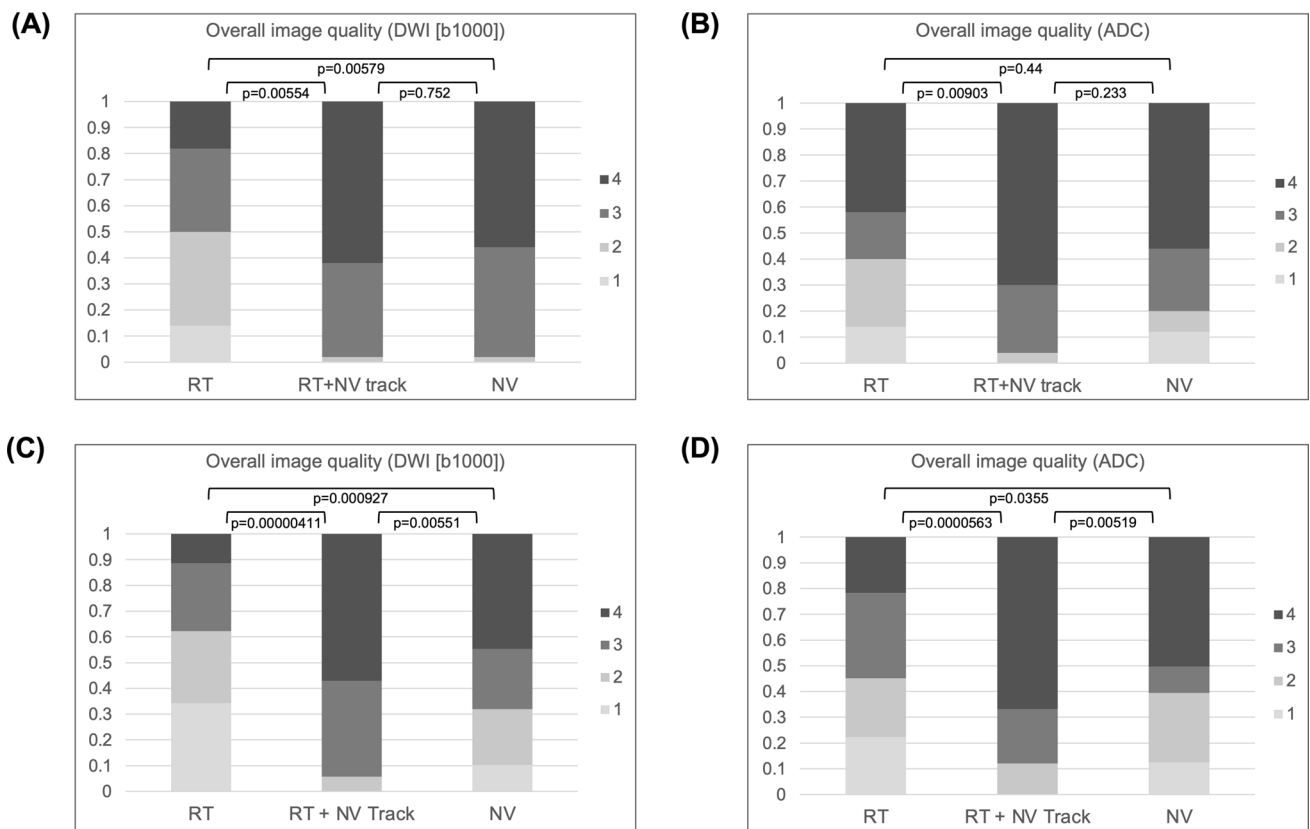
Fig. 5 Qualitative image analysis results (**A**, **B**: Volunteer study; **C**, **D**: Clinical study). In the overall image quality of the DWI (b1000) images in the volunteer study (**A**), RT+NV Track and NV were rated significantly higher than RT ($p=0.00554$, 0.00579). RT+NV Track was rated slightly higher than NV, but the difference was not significant ($p=0.752$). In the overall image quality of ADC images in the volunteer study (**B**), RT+NV Track was rated significantly higher than RT ($p=0.00903$). RT+NV Track was rated higher than NV, but the difference was not significant ($p=0.233$). There
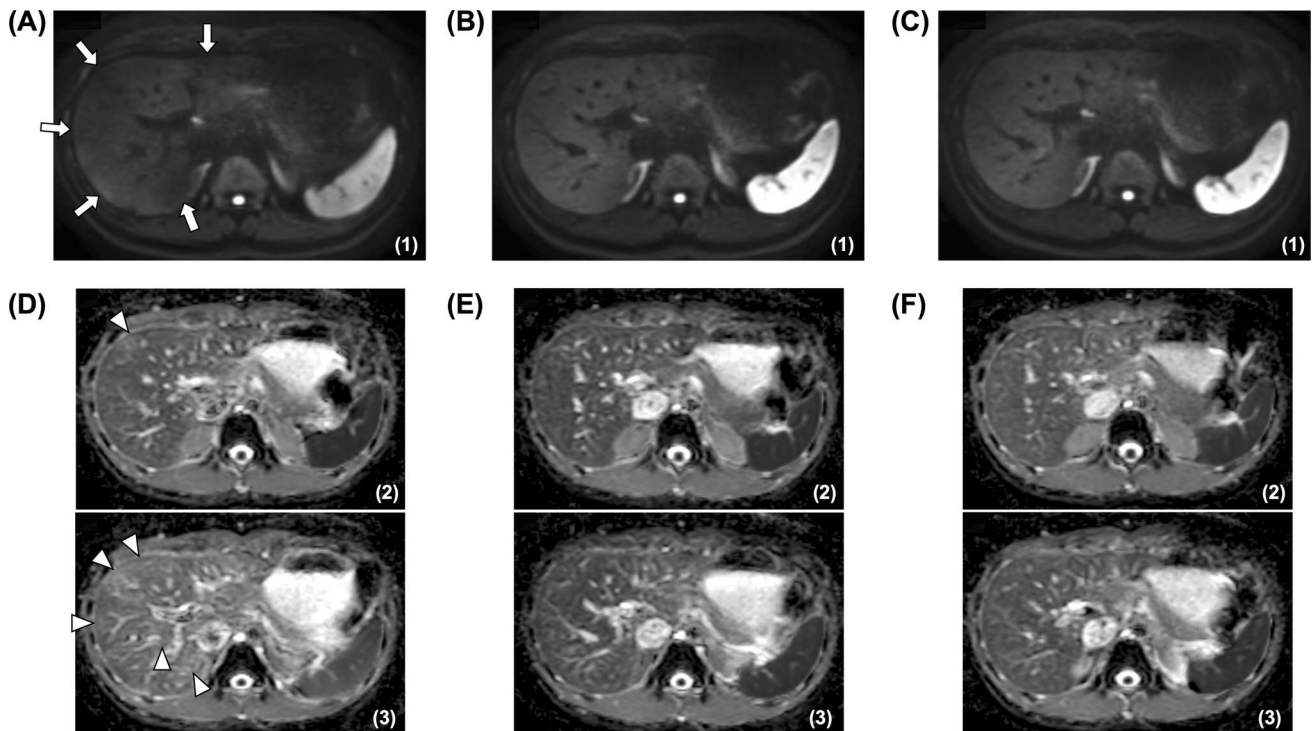
was no significant difference between RT and NV ($p=0.44$). In the overall image quality of DWI (b1000) images in the clinical study (**C**), RT+NV Track was rated significantly higher than RT and NV ($p=0.00000411$, 0.00551). NV was rated significantly higher than RT ($p=0.000927$). In the overall image quality of ADC images in the clinical study (**D**), RT+NV Track was also significantly higher than RT and NV ($p=0.0000563$, 0.00519). NV was rated significantly higher than RT ($p=0.0355$)

On the other hand, RT + NV Track was slightly higher than NV, but the difference was not significant (4 [2−4], 4 3.6 ± 0.23 vs 4 [2−4], 4; $p = 0.752$) (Fig. 5A). In the evaluation of ADC images, RT + NV Track was significantly higher than RT (4 [2−4], 4 vs 3 [1−4], 4; $p < 0.01$). On the other hand, RT + NV Track was higher than NV, but the difference was not significant (4 [2−4], 4 vs 4 [1−4], 4; $p = 0.233$) (Fig. 5B).

Representative images of a volunteer are shown in Fig. 6 (Supporting Information Video S4). In the DWI (b1000) images, RT showed poor image quality due to variations in the depth of respiration (arrows), whereas RT + NV Track and NV showed good image quality (Fig. 6A–C). In the ADC images, uneven liver signal intensity was observed between slices in RT (arrowheads), but RT + NV Track and NV showed good image quality without uneven liver signal intensity (Fig. 6D–F).

Clinical study

All data were successfully acquired. RT + NV Track and RT were comparable in actual imaging time (155.3 ± 24.39 s vs 158.0 ± 26.24 s; $p = 0.305$). In contrast, RT + NV Track was significantly shorter than NV in actual imaging time (155.3 ± 24.39 s vs 227.1 ± 58.86 s; $p < 0.001$). The results of the quantitative image analysis are shown in Fig. 7A–D. In $SNR_{efficiency}$, RT was significantly higher than NV in all four liver ROIs ([ROI1] 12.05 ± 4.65 1/$min^{1/2}$ vs 10.05 ± 3.18 1/$min^{1/2}$; $p < 0.01$, [ROI2] 12.03 ± 4.31 1/$min^{1/2}$ vs 9.82 ± 2.86 1/$min^{1/2}$; $p < 0.001$, [ROI3] 12.60 ± 5.03 1/$min^{1/2}$ vs 9.73 ± 2.61 1/$min^{1/2}$; $p < 0.001$, [ROI4] 13.11 ± 5.54 1/$min^{1/2}$ vs 10.68 ± 4.08 1/$min^{1/2}$; $p < 0.001$) (Fig. 7A–D). Moreover, RT + NV Track was significantly higher than RT and NV in all four ROIs of the liver ([ROI1] 14.01 ± 4.86 1/$min^{1/2}$; $p < 0.001$, $p < 0.001$, [ROI2] 14.09 ± 5.79 1/

Fig. 6 RT (**A**: DWI [b1000], **D**: ADC), RT+NV Track (**B**: DWI [b1000], **E**: ADC), and NV (**C**: DWI [b1000], **F**: ADC) images in a healthy volunteer. In the DWI (b1000) image, image quality degraded in RT due to variations in the depth of respiration (arrow) (**A**). RT+NV Track and NV improved image quality and provided good images (**B**, **C**). In ADC images, RT showed uneven liver signal intensity between slices (arrowheads) (**D**). In RT+NV Track and NV, no uneven liver signal intensity was observed between slices, and good image quality was acquired (**E**, **F**). Actual scan duration; RT: 2 min 24 s, RT+NV Track: 2 min 36 s, NV: 3 min 11 s

$min^{1/2}$; $p < 0.001$, $p < 0.001$, [ROI3] 14.26 ± 5.87 $1/min^{1/2}$; $p < 0.001$, $p < 0.001$, [ROI4] 14.95 ± 5.76 $1/min^{1/2}$; $p < 0.001$, $p < 0.001$) (Fig. 7A–D).

In the CV of ADC values, NV was significantly lower than RT in all four points of the liver ([ROI1] 0.057 ± 0.034 vs 0.080 ± 0.042; $p < 0.001$, [ROI2] 0.054 ± 0.024 vs 0.076 ± 0.034; $p < 0.001$, [ROI3] 0.059 ± 0.032 vs 0.077 ± 0.046; $p < 0.01$, [ROI4] 0.059 ± 0.032 vs 0.075 ± 0.035; $p < 0.01$). Furthermore, RT+NV Track was significantly lower than RT and NV in all four points of the liver ([ROI1] 0.033 ± 0.018; $p < 0.001$, $p < 0.001$, [ROI2] 0.033 ± 0.017; $p < 0.001$, $p < 0.001$, [ROI3] 0.038 ± 0.022; $p < 0.001$, $p < 0.001$, [ROI4] 0.033 ± 0.019; $p < 0.001$, $p < 0.001$) (Fig. 7E–H).

The results of the qualitative image analysis are shown in Fig. 5C, D. Moreover, the results of qualitative image analysis are shown below as (Median value [Minimum value—Maximum value], Mode value). In the evaluation of DWI (b1000) images, RT+NV Track was significantly higher than RT and NV (4 [2−4], 4 vs 2 [1−4], 1, 3 [1−4], 4; $p < 0.001$, $p < 0.01$) (Fig. 5C). RT+NV Track was also significantly higher than RT and NV in the evaluation of ADC images (4 [2−4], 4 vs 3 [1−4], 3, 4 [1 − 4], 4; $p < 0.001$, $p < 0.01$) (Fig. 5D).

Clinical case

Figure 8 shows upper abdominal DWI and ADC images using RT, NV, and RT+NV Track in a patient with suspected gallbladder polyps. In the DWI (b1000) images, RT showed artifacts due to poor fat suppression in the third and fourth slices from the beginning of excitation (arrows), whereas RT+NV Track improved the poor fat suppression and provided good image quality without artifacts (Fig. 8A, C). NV significantly increased the scan time due to poor reading of the navigator, which raised the trigger position (blue line) and prevented data acquisition many times (Supporting Information Fig. S2). In addition, NV included inspiratory data in the data acquisition, resulting in lower image quality at the superior margin of the liver compared to RT and RT+NV Track (arrowheads) (Fig. 8E). In ADC images, RT and RT+NV Track provided good image quality (Fig. 8B, D). On the other hand, NV showed uneven liver signal intensity between slices (yellow dashed arrows), and two sequential slices were the same position images due to the slice misregistration caused by respiratory variation because the data acquisition included inspiratory data (Fig. 8F; Supporting Information Video S5).
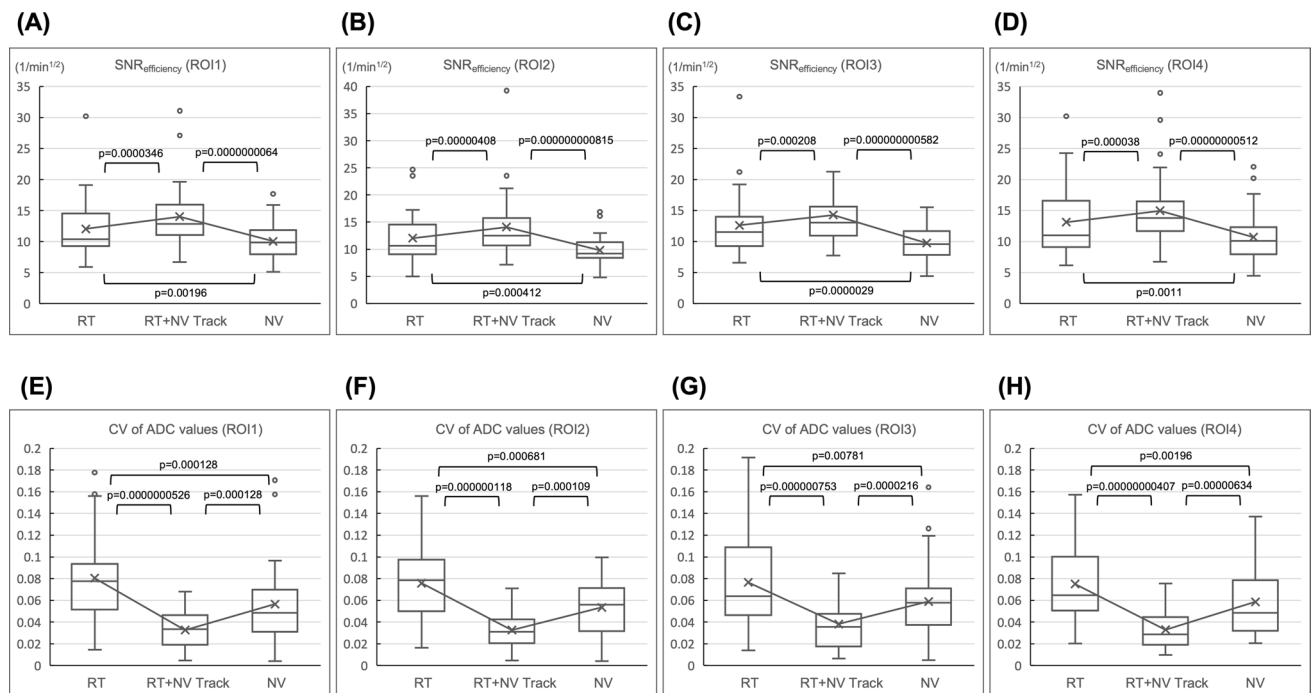
Fig. 7 Quantitative image analysis results of the clinical study. In DWI(b1000) images, the $SNR_{efficiency}$ of RT + NV Track was significantly higher than RT and NV in all ROI1 (**A**), ROI2 (**B**), ROI3 (**C**), and ROI4 (**D**) ([ROI1] $p = 0.0000346$, 0.000000000064, [ROI2] $p = 0.00000408$, 0.000000000815, [ROI3] $p = 0.000208$, 0.000000000582, [ROI4] $p = p = 0.000038$, 0.00000000512). The SNRefficiency of RT was significantly higher than NV in all four ROIs. In CV of ADC values, RT + NV Track was significantly lower than NV and RT in all ROI1 (**E**), ROI2 (**F**), ROI3 (**G**), and ROI4 (**H**) ([ROI1] $p = 0.0000000526$, 0.000128, [ROI2] $p = 0.000000118$, 0. 000109, [ROI3] $p = 0.000000753$, 0.0000216, [ROI4] $p = 0.000000407$, 0.00000634). The CV of the ADC values of NV was significantly lower than RT in all four ROIs

Figures 9 and 10 show upper abdominal DWI and ADC images using RT, NV, and RT + NV Track in a patient with multiple liver metastases with rapid breathing and respiratory variability (Supporting Information Fig. S3). In the DWI (b1000) images, RT showed significant degradation in image quality due to respiratory variability, especially in the kidney signal intensity unevenness between slices (arrows) (Fig. 9A). RT + NV Track corrected for respiratory variations, resulting in improved image quality and good image quality without signal intensity unevenness (Figs. 9C and 10C). NV also showed good image quality (Figs. 9E and 10E). In the ADC images, RT showed uneven signal intensity in the kidneys and liver between slices due to respiratory variations (dashed arrows) (Fig. 9B; Supporting Information Video S6). RT + NV Track corrected for respiratory variations, resulting in improved image quality and good image quality without signal intensity unevenness (Figs. 9D and 10D). NV showed significant signal intensity unevenness in the liver lesion and spleen (arrowhead) due to the inclusion of inspiratory data in the data acquisitions because of rapid breathing (Fig. 10F; Supporting Information Video S6).

Discussion

We have developed a new motion correction method for upper abdominal DWI named RT + NV Track, which combines RT using a respiration sensor and NV Track using navigator echoes to correct slice position misregistration due to respiratory variation at the diaphragm position. In volunteer and clinical studies, RT + NV Track was superior to RT and NV in the evaluation of $SNR_{efficiency}$. In the CV of ADC values and visual evaluation, the image quality of RT + NV Track was superior to RT, comparable to NV in the volunteer study, and superior to NV in the clinical study. This means RT + NV Track is an efficient imaging method that can stably provide good images in a short scan time.

In the evaluation of $SNR_{efficiency}$, we consider that the RT method uses only the motion of the abdominal wall to synchronize respiration for imaging, and thus the variations in the depth of respiration are directly affected, resulting in lower $SNR_{efficiency}$ due to the lower SNR of the liver caused by the degradation of the image quality. Moreover, the NV caused increased actual scan
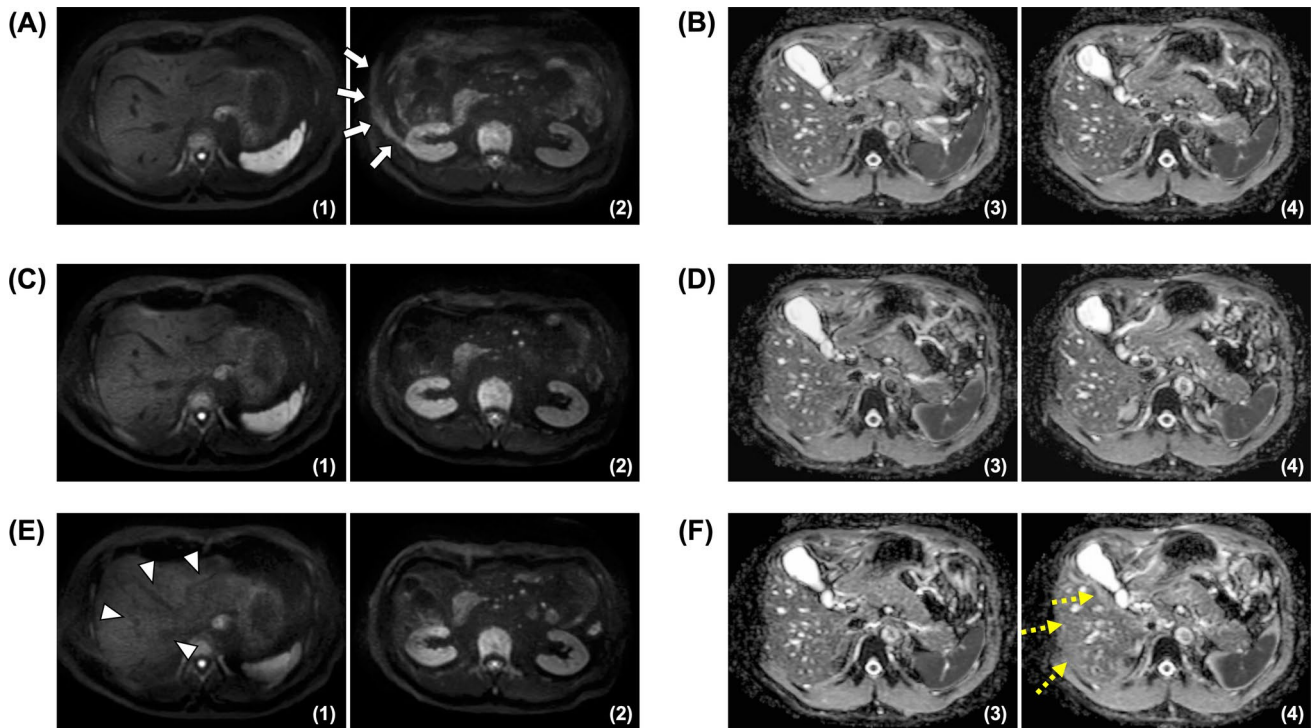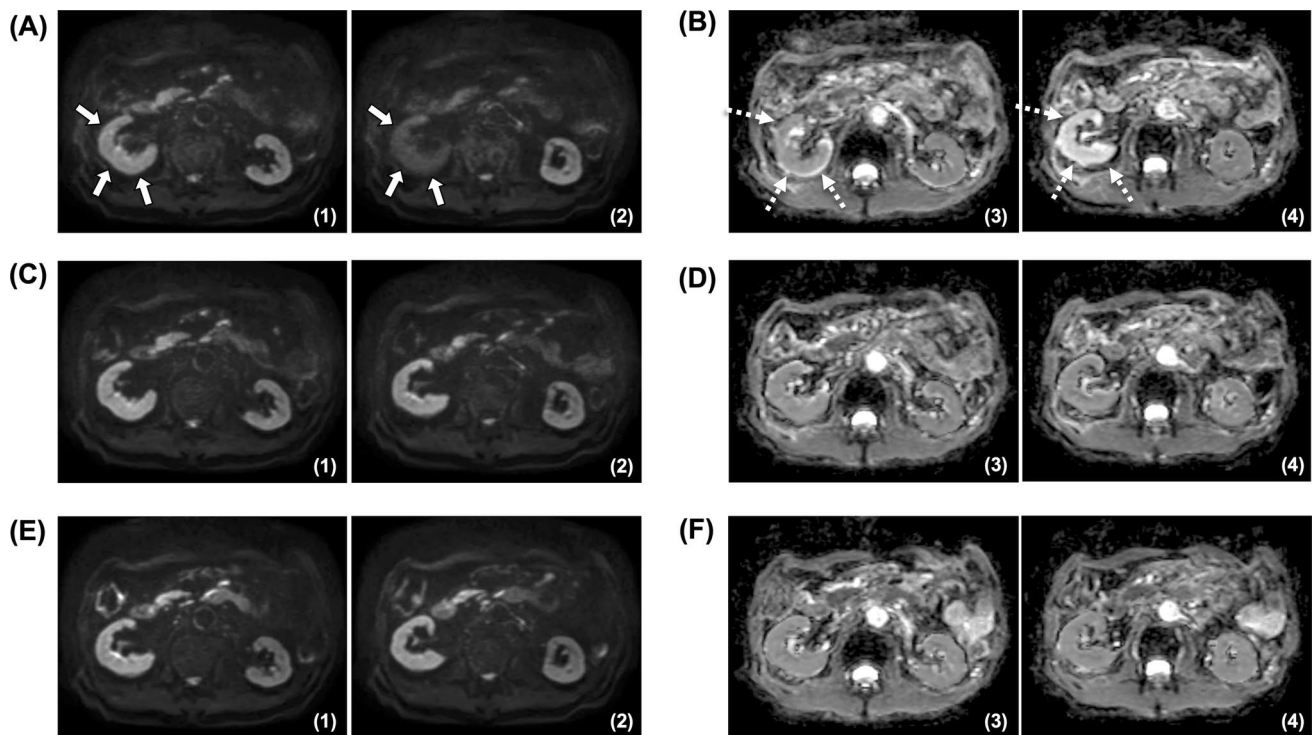
Fig. 8 RT (**A**: DWI [b1000], **B**: ADC), RT+NV Track (**C**: DWI [b1000] **D**: ADC), and NV (**E**: DWI [b1000], **F**: ADC) images for a patient with suspected gallbladder polyps. In the DWI (b1000) image, NV (**E** [1]) had poorer image quality at the superior margin of the liver than RT (**A** [1]) and RT+NV Track (C [1]) due to the inclusion of inspiratory data in the data acquisition (arrowheads). Furthermore, RT (**A** [2]) showed artifacts due to poor fat suppression (arrows), whereas RT+NV Track (**C** [2]) and NV (**E** [2]) improved the poor fat suppression and provided good image quality without artifacts. In ADC images, good image quality was acquired with RT (**B**) and RT+NV Track (**D**). On the other hand, NV (**F**) showed uneven liver signal intensity between slices (yellow dashed arrows) (**F** [4]) and two sequential slices were the same position slice images (**F** [3, 4]) due to the slice misregistration caused by the inclusion of inspiratory data in the data acquisition. Actual scan duration; RT: 3min46sec, RT+NV Track: 3 min 34 s, NV: 6 min 16 s

time due to the inability to acquire data because of the poor reading of the navigator and changes in triggering position caused by the inhomogeneity of the magnetic field. The NV also sometimes included inspiratory data in the data acquisition, resulting in lower image quality and lower SNR for the liver. In particular, we observed that patients in the clinical studies had more respiratory turbulence during imaging than healthy volunteers, causing inaccurate trigger positioning and tracking in NV, increasing the actual imaging time and often introducing inspiratory data into the data acquisition. We consider that the $SNR_{efficiency}$ of NV was decreased due to these increased actual scan times and lower SNR of the liver. On the other hand, RT+NV Track does not cause failure to acquire data due to poor reading of the navigator and does not increase the actual scan time because it uses the motion of the abdominal wall to synchronize respiration for imaging. In addition, RT+NV Track tends to acquire only expiratory data even in patients with relatively rapid breathing (Figs. 9C and 10C) because the time to begin data acquisition is earlier when synchronizing with the motion of the abdominal wall than with the diaphragm.

Furthermore, RT+NV Track can correct for respiratory variability at the diaphragm position using NV Track, thus minimizing image quality degradation due to variations in the depth of respiration. For these reasons, the $SNR_{efficiency}$ of RT+NV Track was significantly higher than the conventional method.

In the evaluation of the CV of ADC values, RT caused misregistrations between low b-value (b-value = 0 s/mm²) and high b-value (b-value = 1000 s/mm²) images due to variations in the depth of respiration, and the difficulty in obtaining accurate ADC images could be attributed to the variations in ADC values between slices. On the other hand, NV and RT+NV Track are triggered or corrected at the diaphragm position, resulting in less misregistration between low b value (b value 0 s/mm²) and high b value (b value 1000 s/mm²) images, which may have stabilized ADC values between slices relatively. However, especially in patients in clinical studies, NV often included inspiratory data in the data acquisitions due to poor navigator readings by magnetic field inhomogeneity or inaccurate trigger position setting and tracking due to respiratory turbulence. Moreover, NV also often included inspiratory data in data acquisition of

Fig. 9 RT (**A**: DWI [b1000], **B**: ADC) and RT + NV Track (**C**: DWI [b1000] **D**: ADC), and NV (**E**: DWI [b1000], **F**: ADC) images of kidney-level slices in a patient with multiple liver metastases with rapid breathing and respiratory variability. RT showed significant kidney signal intensity unevenness between slices (arrows, dashed arrows) (**A**, **B**) in both DWI (b1000) and ADC images due to respiration variability. RT + NV Track improves the image quality of both DWI (b1000) and ADC images by correcting for respiratory variations, resulting in good image quality without signal intensity unevenness (**C**, **D**). NV also showed good image quality for both DWI (b1000) and ADC images (**E**, **F**). Actual scan duration; RT: 2 min 22 s, RT + NV Track: 2 min 15 s, NV: 3 min 37 s

subjects with rapid breathing, and accurate ADC images were difficult to obtain due to respiratory misregistration between low b value (b value $= 0$ s/mm^2) and high b value (b value $= 1000$ s/mm^2) images. For these reasons, NV may have had a larger CV of ADC values between slices than RT + NV Track.

In fat suppression of DWI (b1000) images, the navigator is run multiple times as the preparation for reading the navigator prior to data acquisition in the NV method. Spectral presaturation with inversion recovery (SPIR) is used in conjunction with these preparation navigators in the MR scanner used in this study. In other words, SPIR is irradiated many times before data acquisition; thus, NV showed good fat suppression even in multiple slices at the beginning of the excitation. On the other hand, the navigator preparation is not run in the RT method; thus, the first SPIR is irradiated at the start of data acquisition. The RF pulse flip angle in SPIR of the MR scanner used in this study is set to the 91° optimized flip angle for the first slice of each package and the 100° flip angle for the second and subsequent slices in the RT method of the abdomen. In this study, because the package was 2, the slices were divided into [1, 3, 5, 7, 9,…] and [2, 4, 6, 8, 10,…], and excited sequentially. Poor fat suppressions were observed at slice-3,4 in RT, in other words, at the second slice of each package. In slice-1,2, although the longitudinal magnetization of fat was not yet stable, the RF pulse flip angle of SPIR was set at a shallow and optimized angle of 91°, thus considering that the null point of fat could be easily matched and fat suppression was good. However, in slice-3,4, although the longitudinal magnetization of fat was not yet stable, the RF pulse flip angle of SPIR was 100°, thus considering that the null point of fat was not easily matched and fat suppression was not successful (Table 2A). In the RT + NV Track method, navigator preparation is not performed, but the data acquisition is triggered by the respiratory waveform due to abdominal wall motion and is performed after NV Track is performed. The NV Track is also used with SPIR on the MR scanner used in this study. Therefore, slices-3,4, which showed poor fat suppression in RT, were irradiated with SPIR for actually the fourth time in RT + NV Track, which in effect, stabilized the longitudinal magnetization of fat and probably resulted in good fat suppression even with a flip angle of 100° for the RF pulse of SPIR (Table 2B). For this reason, RT + NV Track may have improved artifacts caused by poor fat suppression. This study shows that RT + NV
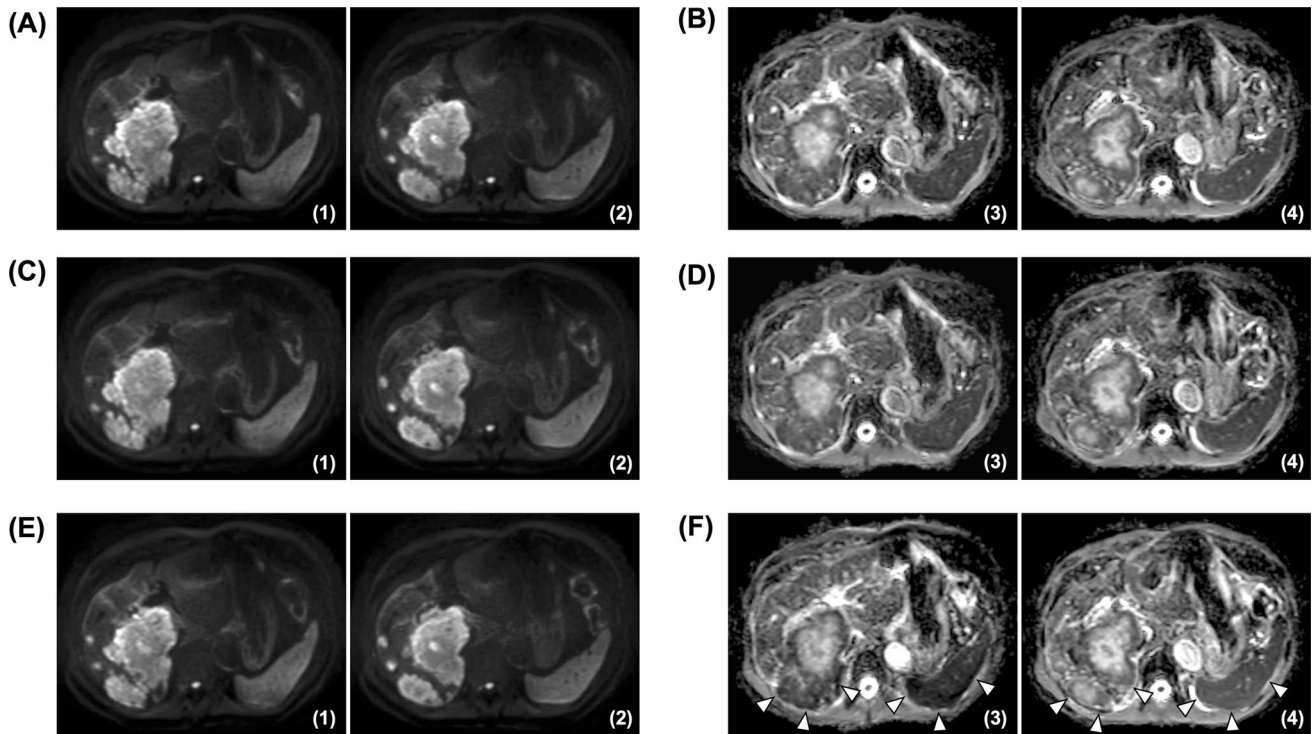
Fig. 10 RT (**A**: DWI [b1000], **B**: ADC), RT + NV Track (**C**: DWI [b1000], **D**: ADC), and NV (**E**: DWI [b1000], **F**: ADC) images of liver-spleen level slices in a patient with multiple liver metastases with rapid breathing and respiratory variability. RT, RT + NV Track, and NV all showed good image quality in the DWI (b1000) images (**A**, **C**, **E**). However, in ADC images, NV showed significant signal intensity unevenness in the liver lesion and spleen between slices (arrowhead) due to the inclusion of inspiratory data in the data acquisition because of rapid breathing (**E**). RT + NV Track tended to acquire only expiratory data even in patients with relatively rapid breathing, and improved image quality by correcting for respiratory variability, resulting in good image quality without signal intensity unevenness (**D**). RT showed good image quality at the liver-spleen level slices (**B**). Actual scan duration; RT: 2min22sec, RT + NV Track: 2 min 15 s, NV: 3 min 37 s

Table 2 Relationship between the number of SPIR irradiations and the effect of fat suppression in the RT method (A) and the RT + NV Track method (B)

	A			B		
	RT			RT + NV Track		
Number of SPIR irradiations	Slice	RF-pulse flip angle in SPIR	Fat suppression efficacy	Slice	RF-pulse flip angle in SPIR	Fat suppression efficacy
1st	1,2	91° (Optimized angle)	good	NV Track	91° (Optimized angle)	Unrelated to image
2nd	3,4	100°	poor	1,2	91°	good
3rd	5,6	100°	good	NV Track	100°	Unrelated to image
4th	7,8	100°	good	3,4	100°	good
5th	9,10	100°	good	NV Track	100°	Unrelated to image
6th	11,12	100°	good	5,6	100°	good

Track is a hybrid method combining the advantages of both RT and NV. The RT + NV Track method, which can improve the image quality degradation of conventional methods and obtain consistently and efficiently good images, has potential for further applications. Advanced DWI approaches such as IVIM experiments and Kurtosis DWI are often used in the liver [34]. Even in these advanced DWI approaches, RT + NV Track may be as effective as in this study, since imaging that requires many b values is more susceptible to misregistration due to respiration.

The RT + NV Track method and our present study have a few limitations. First, because the RT + NV Track method uses respiratory triggering, in thin subjects, the respiratory sensor may detect not only the motion of the abdominal wall by respiration but also the pulsations of the abdominal aorta. When the respiratory waveform is disturbed due to the pulsations of the abdominal aorta, the triggering may occur at the wrong timing, which is not expiration, and even the correction of respiratory variation with NV Track may not be able to fully correct the problem, resulting in degradation of the image quality. However, the influence of abdominal aortic pulsations can be minimized by carefully positioning the respiratory sensor to avoid the pulsations of the abdominal aorta during the positioning of the subject before the start of the examination. Furthermore, VitalEye [35, 36] has recently been reported as a camera-based respiratory navigation sensor technique. This state-of-the-art technology enables non-contact respiratory monitoring without conventional respiratory sensors, thus avoiding false detection of abdominal aortic pulsations. In the future, combining the RT + NV Track method with a camera-based respiratory navigation sensor could provide a motion compensation technique that is more robust to respiratory variability. Second, the SPIR was used for fat suppression in this study. The RT method showed poor fat suppression in the second slice of each package, and the RT + NV Track method improved the fat suppression, but the results may differ from those of this study if Spectral Attenuated Inversion Recovery (SPAIR) is used for fat suppression. However, when SPAIR is used for DWI in the RT method, it has been previously reported that poor fat suppression is observed in several slices at the beginning of excitation [37]. In addition, the combination of RT + NV Track and SPAIR could not be used with the MR scanner in this study. However, because the RT + NV Track method provided good fat suppression in all subjects in this study, we consider that SPAIR is not necessary and SPIR is sufficient. Furthermore, although this study was performed at 3.0 T, the proposed RT + NV Track method can be easily extended to 1.5 T, with fewer challenges in magnetic field uniformity.

Conclusion

The RT + NV Track method improves image quality degradation due to respiratory variability and poor fat suppression compared to the conventional method of RT. Furthermore, the RT + NV Track method has a shorter actual scan time than the conventional method of NV and can be applied to patients with rapid breathing. In other words, RT + NV Track is an efficient imaging method for upper abdominal DWI that can obtain consistently good images in a short time. RT + NV Track method can be the first choice of motion correction technique in upper abdominal DWI.

Declarations

Conflict of interest Hiroshi Hamano is an employee of Philips Japan.

Ethical statement The study was approved by the institutional review board, and written informed consent was obtained from all subjects. Approval number: 22I-0302-004.

References

1. Vilgrain V, Esvan M, Ronot M, Caumont-Prim A, Aubé C, Chatellier G (2016) A meta-analysis of diffusion-weighted and gadoxetic acid-enhanced MR imaging for the detection of liver metastases. Eur Radiol 26:4595–4615
2. Katsuhiro N, Kuroki Y, Nawano S et al (2006) Hepatic metastases: diffusion-weighted sensitivity-encoding versus SPIO-enhanced MR imaging. Radiology 239:122–130
3. Taouli B, Koh D-M (2010) Diffusion-weighted MR Imaging of the liver. Radiology 254:47–66
4. Piana G, Trinquart L, Meskine N, Barrau V, Van Beers B, Vilgrain V (2011) New MR imaging criteria with a diffusion-weighted sequence for the diagnosis of hepatocellular carcinoma in chronic liver diseases. J Hepatol 55:126–132
5. Vandecaveye V, De Keyzer F, Verslype C et al (2009) Diffusion-weighted MRI provides additional value to conventional dynamic contrast-enhanced MRI for detection of hepatocellular carcinoma. Eur Radiol 19:2456–2466
6. American College of Radiology. Liver Reporting & Data System (LI-RADS®) https://www.acr.org/Clinical-Resources/Reporting-and-Data-Systems/LI-RADS%0A%0A. Accessed: 18 Aug 2022
7. Van Den Bos IC, Hussain SM, Krestin GP, Wielopolski PA (2008) Liver imaging at 3.0 T: Diffusion-induced black-blood echo-planar imaging with large anatomic volumetric coverage as an alternative for specific absorption rate-intensive echo-train spin-echo sequences: feasibility study. Radiology 248:264–271
8. Coenegrachts K, Delanote J, Ter Beek L et al (2007) Improved focal liver lesion detection: comparison of single-shot diffusion-weighted echoplanar and single-shot T2 weighted turbo spin echo techniques. Br J Radiol 80:524–531
9. De Robertis R, Tinazzi Martini P, Demozzi E et al (2015) Diffusion-weighted imaging of pancreatic cancer. World J Radiol 7:319–328
10. d'Assignies G, Fina P, Bruno O et al (2013) High sensitivity of diffusion-weighted mr imaging for the detection of liver metastases from neuroendocrine tumors: comparison with t2-weighted and dynamic gadolinium-enhanced mr imaging. Radiology 268:390–399
11. Roth Y, Tichler T, Kostenich G et al (2004) High-*b* value diffusion-weighted MR imaging for pretreatment prediction and early monitoring of tumor response to therapy in mice. Radiology 232:685–692

12. Obara M, Kwon J, Yoneyama M et al (2023) Technical advancements in abdominal diffusion-weighted imaging. Magn Reson Med Sci 22:191–208

13. Naganawa S, Kawai H, Fukatsu H et al (2005) Diffusion-weighted imaging of the liver: technical challenges and prospects for the future. Magn Reson Med Sci 4:175–186

14. Ichikawa T, Haradome H, Hachiya J et al (1998) Diffusion-weighted MR imaging with a single-shot echoplanar sequence: detection and characterization of focal hepatic lesions. AJR Am J Roentgenol 170:397–402

15. Taouli B, Chouli M, Martin AJ et al (2008) Chronic hepatitis: role of diffusion-weighted imaging and diffusion tensor imaging for the diagnosis of liver fibrosis and inflammation. J Magn Reson Imaging 28:89–95

16. Girometti R, Furlan A, Bazzocchi M et al (2007) Diffusion-weighted MRI in evaluating liver fibrosis: a feasibility study in cirrhotic patients. Radiol Med (Torino) 112:394–408

17. Parikh T, Drew SJ, Lee VS et al (2008) Focal liver lesion detection and characterization with diffusion-weighted MR imaging: comparison with standard breath-hold T2-weighted imaging. Radiology 246:812–822

18. Choi JS et al (2013) Comparison of breathhold, navigator-triggered, and free-breathing diffusion-weighted MRI for focal hepatic lesions. J Magn Reson Imaging 38:109–118

19. Kwee TC, Takahara T, Koh DM, Nievelstein RAJ, Luijten PR (2008) Comparison and reproducibility of ADC measurements in breathhold, respiratory triggered, and free-breathing diffusion-weighted MR imaging of the liver. J Magn Reson Imaging 28:1141–1148

20. Takayama Y, Nishie A, Asayama Y et al (2015) Optimization and clinical feasibility of free-breathing diffusion-weighted imaging of the liver: comparison with respiratory-triggered diffusion-weighted imaging. Magn Reson Med Sci 14:123–132

21. Chen X, Qin L, Pan D et al (2014) Liver diffusion-weighted MR imaging: reproducibility comparison of ADC measurements obtained with multiple breath-hold, free-breathing, respiratory-triggered, and navigator-triggered techniques. Radiology 271(1):113–125

22. Xie S, Masokano IB, Liu W et al (2021) Comparing the clinical utility of single-shot echo-planar imaging and readout-segmented echo-planar imaging in diffusion-weighted imaging of the liver at 3 tesla. Eur J Radiol 135:109472

23. Bruegel M, Holzapfel K, Gaa J et al (2008) Characterization of focal liver lesions by ADC measurements using a respiratory triggered diffusion-weighted single-shot echo-planar MR imaging technique. Eur Radiol 18:477–485

24. Nasu K, Kuroki Y, Sekiguchi R, Nawano S (2006) The effect of simultaneous use of respiratory triggering in diffusion-weighted imaging of the liver. Magn Reson Med Sci 5:129–136

25. Kandpal H, Sharma R, Madhusudhan KS, Kapoor KS (2009) Respiratory-triggered versus breath-hold diffusion-weighted MRI of liver lesions: comparison of image quality and apparent diffusion coefficient values. AJR Am J Roentgenol 192:915–922

26. Taouli B, Sandberg A, Stemmer A et al (2009) Diffusion-weighted imaging of the liver: comparison of navigator triggered and breathhold acquisitions. J Magn Reson Imaging 30:561–568

27. Gourtsoyianni S, Papanikolaou N, Yarmenitis S et al (2008) Respiratory gated diffusion-weighted imaging of the liver: value of apparent diffusion coefficient measurements in the differentiation between most commonly encountered benign and malignant focal liver lesions. Eur Radiol 18:486–492

28. Choi JS, Kim MJ, Chung YE et al (2013) Comparison of breath-hold, navigator-triggered, and free-breathing diffusion-weighted MRI for focal hepatic lesions. J Magn Reson Imaging 38:109–118

29. Li C, Magland JF, Rad HS et al (2012) Comparison of optimized soft-tissue suppression schemes for ultra-short echo time (UTE) MRI. Magn Reson Med 68:680–689

30. Mürtz P, Flacke S, Träber F et al (2002) Abdomen: diffusion-weighted MR imaging with pulse-triggered single-shot sequences. Radiology 224:258–264

31. Nasu K, Kuroki Y, Sekiguchi R et al (2006) Measurement of the apparent diffusion coefficient in the liver: is it a reliable index for hepatic disease diagnosis? Radiat Med 24:438–444

32. Kandpal H, Sharma R, Madhusudhan KS et al (2009) Respiratory-triggered versus breath-hold diffusion-weighted MRI of liver lesions: comparison of image quality and apparent diffusion coefficient values. AJR Am J Roentgenol 192:915–922

33. Wang YXJ, Huang H, Zheng CJ et al (2021) Diffusion-weighted MRI of the liver: challenges and some solutions for the quantification of apparent diffusion coefficient and intravoxel incoherent motion. Am J Nucl Med Mol Imaging 11(2):107–142

34. Kartalis N, Manikis GC, Loizou L et al (2016) Diffusion-weighted MR imaging of pancreatic cancer: a comparison of mono-exponential, bi-exponential and non-Gaussian kurtosis models. Eur J Radiol Open 3:79–85

35. Sénégas J, Krueger S, Wirtz D, et al. (2018) Comparison of liver motion measured by dynamic MRI and respiration signals obtained by an optical sensor. In: Proceedings of the 26th annual meeting Intl Soc Mag Reson Med (ISMRM), Paris. p. 2528.

36. Harder F, Lohöfer FK, Kaissis GA et al (2019) Camera-based respiratory triggering improves the image quality of 3D magnetic resonance cholangiopancreatography. Eur J Radiol 120:108675

37. Takano S, Horie T, Endo K et al (2013) Problem of spectral attenuated with inversion recovery fat suppression method with respiratory-gated. Jpn J Radiol Technol 61:92–98. https://doi.org/10.6009/jjrt.2013_JSRT_69.1.92